Journal of Organometallic Chemistry, 415 (1991) 167–180
Elsevier Sequoia S.A., Lausanne
JOM 21983

Structural studies of organometallic compounds in solution

IV *. An extended X-ray absorption fine structure (EXAFS) and large angle X-ray scattering (LAXS) study of organomagnesium bromides in diethyl ether

Agneta Wellmar [a], Anders Hallberg [b] and Ingmar Persson [c,*]

[a] *Inorganic Chemistry 1, Chemical Centre, University of Lund, P.O. Box 124, S-221 00 Lund (Sweden)*
[b] *Department of Organic Pharmaceutical Chemistry, Uppsala University, P.O. Box 574, S-751 23 Uppsala (Sweden)*
[c] *Department of Chemistry, Swedish University of Agricultural Sciences, P.O. Box 7015, S-750 07 Uppsala (Sweden)*

(Received March 25th, 1991)

Abstract

Phenylmagnesium bromide in diethyl ether solution has been studied by large angle X-ray scattering (LAXS) and extended X-ray absorption fine structure, EXAFS, techniques. The reagent is present as both dimeric and monomeric complexes in this solvent, with magnesium octahedrally coordinated in both cases. The Mg–Br bond distance is 2.56(2) Å and the Br–Br bond distance in the dimeric complex is 3.62(3) Å. The local structure around bromine in methyl- and ethyl-magnesium bromides has also been determined in diethyl ether solution by EXAFS. Data for the Br K edge were collected for solutions in the concentration range 0.1-1.0 *M*. For all the solutions the Mg–Br bond distance was found to be the same, 2.54 Å, within the limits of error. No other interaction was observed.

Introduction

Grignard compounds are important reagents in organic synthesis [1]. One of the most investigated reactions is that of alkyl- or aryl-magnesium halides with aldehydes and ketones; the current view is that this reaction proceeds via an electron transfer mechanism [2]. A four-centered cyclic transition state has also been suggested [3].

Grignard reactions are difficult to study since there are a variety of species present in solution and since the composition of these solutions depends on the concentration, the solvent, the temperature and the alkyl- or aryl-group attached to the magnesium. Furthermore, the study of these solutions is complicated by the fact

* For Part III see ref. 17.

0022-328X/91/$03.50

that both R_2Mg and RMgX, species possibly present in the Schlenk equilibrium (eq. 1), can react with aldehydes or ketones to form alcohols [4].

$$2\ RMgX \rightleftharpoons R_2Mg + MgX_2 \quad (1)$$

The existence of the Schlenk equilibrium was proposed in 1929 [5]. The equilibrium can be extended further to include dimers:

$$(RMgX)_2 \rightleftharpoons 2\ RMgX \rightleftharpoons R_2Mg + MgX_2 \quad (2)$$

A number of dimeric species can be envisaged and these can be in equilibrium with each other and with monomeric species. The position of the equilibrium is mainly dependent on the solvent used. A more strongly coordinating solvent, such as tetrahydrofuran (THF) favours formation of monomeric RMgX.

Many attempts have been made to determine the structures of the Grignard reagents. The studies have focussed on X-ray diffraction in the solid state. The crystal structure of the phenylmagnesium bromide dietherate has been determined [6]. It was found to be a monomeric complex with magnesium tetrahedrally surrounded by a phenyl group, a bromide ion, and two solvent molecules, Fig. 5. A Mg–Br bond distance of 2.44 Å was observed. In the corresponding ethyl compound [7], which is also monomeric and tetrahedral, the Mg–Br distance is 2.48 Å. The dimeric complex $[EtMgBr \cdot Et_3N]_2$ has been crystallised from triethylamine solution; it has bridging bromide ions in a tetrahedral complex with Mg–Br distances of 2.56 Å [8]. These distances are ca 0.1 Å longer than those in monomeric $MgBr_2(THF)_4$ [9]. In solid $MeMgBr(THF)_3$ the magnesium is five coordinated [10] and at the centre of a trigonal bipyramid. It is apparent that many different crystal structures are possible for Grignard reagents and that no generalisations can be made.

For determining structures in solution various methods have been utilised, e.g. ebullioscopy, IR spectroscopy, and in recent years NMR spectroscopy. Ebullioscopic measurements indicated that the degree of association of the Grignard compounds in diethyl ether, in general, increases with increasing concentration [11]. Conductivity measurements showed that the conductivity decreases with dilution between 2 and 0.5 *M* [12].

The interpretation of IR spectra of diethyl ether solutions of Grignard reagents was inconclusive, but spectra of the corresponding tetrahydrofuran solutions showed that Grignard solutions prepared in this solvent are best represented by a mixture of RMgX, R_2Mg and MgX_2 species, eq. 1 [13]. From a ^{25}Mg NMR study it was suggested that the Schlenk equilibrium exists. For EtMgBr the three species of eq. 1 were detected in THF at 37 °C [14]. A ^1H NMR study was rendered difficult by the rapid intermolecular exchange of alkyl- and aryl-groups at room temperature. At low temperature signals from RMgX and R_2Mg were distinguished [15].

To our knowledge no study has been made of Grignard reagents by extended X-ray absorption fine structure (EXAFS) or large angle X-ray scattering (LAXS) methods. With these techniques valuable information for different types of systems can be obtained [16]. EXAFS spectra provide local structural information about distances and the type and number of atoms surrounding the absorbing atom. It should, in principle, be possible to determine the Br–Mg and Br–Br distances from the measurements. With LAXS the scattering from all the atom pairs present in the solutions is recorded. These techniques could also give information on the number

of Br–Br distances, which would help in determining the proportion of dimeric species probably present in the solutions [17].

We herein report a study of phenylmagnesium bromide in diethyl ether by EXAFS and LAXS methods. This substrate, often used by synthetic chemists and commercially available, was selected because it has been well-characterised in the solid state [6]. Results of an EXAFS study of alkylmagnesium bromides are also discussed.

Experimental

All glass equipment and syringe needles were dried in an oven and all operations were carried out under dry, oxygen-free nitrogen or argon.

Solvents

Anhydrous diethyl ether purchased from Aldrich in Sure/Seal™ bottles was used. The solvent was transferred with hypodermic syringes.

Chemicals

All Grignard reagents were purchased from Aldrich in Sure/Seal™ bottles: ethylmagnesium bromide in diethyl ether, 3 *M*; methylmagnesium bromide in diethyl ether, 3 *M*; phenylmagnesium bromide in diethyl ether, 3 *M*. The reagents were diluted to the desired concentration with anhydrous solvent.

The following compounds were all purchased from Aldrich; Br_2, $KBrO_3$, CBr_4, $MgBr_2$ and NaBr.

Model compounds

The obvious model for Mg back-scattering is $MgBr_2$(s) and data were collected for this compound several times, Table 1. However, due to its very high tendency to absorb water the data were not reproducible and the scans collected could not be

Table 1

EXAFS data collection

Solution		Data collection [a]
CH_3MgBr	0.6 *M*	SSRL1,3
C_2H_5MgBr	0.1 *M*	SSRL1,2,3
	1.0 *M*	SSRL1,2,3,4, SRS
C_6H_5MgBr	0.5 *M*	SSRL1,2,3
	1.0 *M*	SSRL1,3,4
Model		
Br_2		SSRL1,3
CBr_4		SSRL1,3, SRS
BrO_3		SSRL1,2
$MgBr_2$		SSRL1,2,3
NaBr		SSRL4, SRS

[a] SSRL 1 Beam line 7-3, Si(220) double-crystal monochromator, 8-pole wiggler, unfocussed.
SSRL2 Beam line 4-2, Si(111) double-crystal monochromator, 8-pole wiggler, focussing mirror.
SSRL3 Beam line 7-3, Si(111) double-crystal monochromator, 8-pole wiggler, unfocussed.
SSRL4 Beam line 4-1, Si(111) double-crystal monochromator, 8-pole wiggler, unfocussed.
SRS Beam line 9-2, Si(220) double-crystal monochromator, 3-pole wiggler, unfocussed.

averaged. Since hygroscopicity is a problem with all magnesium bromide compounds no suitable magnesium-containing model compound could be found, and solid NaBr was used instead.

Analyses

All the organomagnesium solutions were analysed for magnesium by EDTA titration using Eriochrome Black T as indicator. They were analysed for halide by titration with a standard solution of $AgNO_3$. The analyses were performed in aqueous solution. ^1H NMR spectra were recorded on a Varian XL-300 spectrometer in deuterochloroform for the phenylmagnesium bromide solution before and after the scattering measurements to confirm that the composition of the solution remained unchanged.

LAXS data collection

A large angle θ-θ diffractometer of the Seifert GSD type with Mo-K_α radiation ($\lambda = 0.7107$ Å) was used to measure the scattered intensities from the free surface of the solution [18]. A curved graphite monochromator was placed immediately before the scintillation counter. The solution was kept in a cylindrical, thinwalled glass vessel previously described [19], in order to avoid evaporation and to keep out moisture and air. The container was half-filled. A correction function for the angle dependent absorption by the glass container was determined and applied as described elsewhere [19]. Scattered intensities were collected in the range $4 < \theta < 59°$ with steps of $s = 0.0335$ Å^{-1}, $s = 4\pi \sin\theta\, \lambda^{-1}$. The scattering angle is 2θ. An extrapolation of the intensity data for $\theta < 4°$ was necessary because of the upward liquid meniscus on the glass wall. The reproducibility was checked by repeated scans. 20000 counts were collected for $s < 10.2$ Å^{-1} and 8000 counts for $10.2 \leqslant s \leqslant 15.2$ Å^{-1}. The number of collected counts for $s > 10.2$ Å^{-1} was decreased due to very long counting time. The counting time for each sampling point was never less then 20 min.

LAXS data treatment

Experimental data were initially corrected for background scattering and polarisation effects [18]. Correction for multiple scattering was made because of the low absorption coefficient [20], Table 2. The corrected data were normalised to a stoichiometric volume containing one magnesium atom. The normalisation factor, K, used in the data analysis was derived by comparison of the measured and total independent scattering in the high-angle region, $s > 13$ Å^{-1}. K calculated in this manner was then compared with K calculated according to Krogh-Moe [21] and Norman [22].

Scattering factors, f, for the neutral atoms were used [23] except for H, for which the spherical form factors suggested by Stewart et al. were employed [24]. The

Table 2

Composition of the solution investigated by LAXS

Solution	$[Mg^{2+}]$ (M)	[Solvent] (M)	μ (cm^{-1})
C_6H_5MgBr in diethyl ether	2.0	9.6	13.6

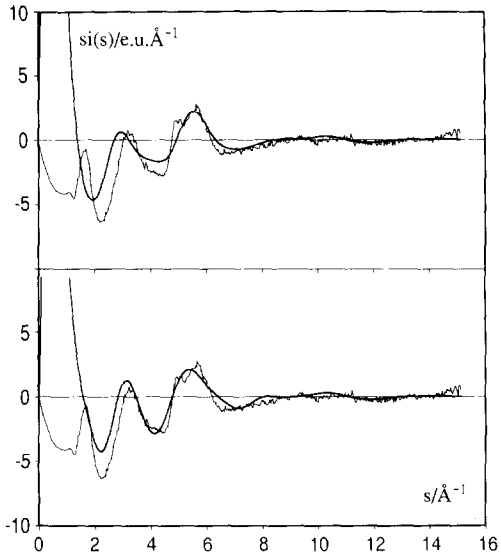

Fig. 1. Reduced intensities, $i(s)$, multiplied by s vs s for 2.0 M phenylmagnesium bromide in diethyl ether solution. The octahedral model is given in the upper part of the figure, and the tetrahedral one in the lower part. Experimental values are represented by the thin line and the values calculated from the final structure model in Table 3 by the thick line.

contribution from anomalous dispersion, $\Delta f'$ and $\Delta f''$, was considered for all atoms [23]. Incoherent scattering factors [25–27], corrected for the Breit–Dirac effect [28,29], were used. The raw data were normal up to s ca 10 Å^{-1}, above which an unexpected decrease in the total intensity was observed. The structural information was, however, not affected by this decrease in intensity. The intensity function was straightened up by applying a smoothed correction function to the experimental data, in such a way that one Fourier transformation was enough to straighten up the entire experimental function, as is the usual case. All these corrections were taken into account when the reduced intensity function, $i(s)$, Fig. 1, and the differential radial distribution functions, $D(R) - 4\pi r^2\rho_0$, Fig. 2, were calculated using standard procedures [30,31]. Spurious peaks below 1.5 Å which could not be identified with interatomic distances in the solutions, were removed by a Fourier transformation procedure [32]. All calculations were made with the program KURVLR [33]. Least-squares refinements were carried out using the STEPLR program [34].

EXAFS data collection and reduction

X-ray absorption spectra were collected at Stanford Synchrotron Radiation Laboratory, SSRL, and at Daresbury Laboratory Synchrotron Radiation Source, SRS. All the solutions, as well as the model compound were measured several times, Table 1. All the experiments were performed under dedicated conditions (3–3.3 GeV, 40 mA, wiggler field at 16.5–18 kG). For the samples as well as the model compounds, bromine K edge EXAFS data were collected in transmission mode with nitrogen-filled ion chambers to monitor incident and transmitted radiation. At SRS the ion chambers were filled with the recommended gas mixture; 19.6 kPa Ar + 81.7 kPa He in the first ion chamber and 15.5 kPa Xe + 85.8 kPa He in the last two ion chambers [35].

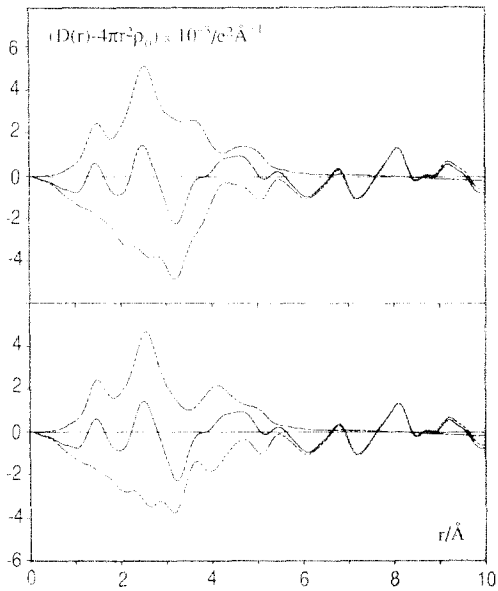

Fig. 2. The differential electronic radial distribution function, $D(r) - 4\pi r^2 \rho_0$, for 2 M phenylmagnesium bromide in diethyl ether solution, solid line. The dashed line represents the sum of the calculated peak shapes and the difference is drawn with a double-dashed line.

The spectra presented represent an average of 2–3 scans. Energy calibration was done by the internal standard technique [36] using KBr film. The inflection point of the KBr standard was assigned as 13472 eV.

The averaged data were reduced by subtracting a smooth polynomial pre-edge extrapolated from a measured pre-edge, subtracting a cubic spline and normalising [37,38]. The spline points were chosen empirically to minimise the residual low-frequency background without reducing the observed amplitude of the EXAFS. The normalised, background-subtracted EXAFS data were converted from energy E to photoelectron wave vector k, $k = [2m_e(E - E_0)/h^2]^{1/2}$, with an E_0 value of 13490 eV. Fourier transforms of the data were calculated by numerical integration with k^3-weighted data.

EXAFS data analyses

The observed EXAFS, $\chi(k)$, can be expressed as

$$\chi(k) = \frac{\sum_i N_i F_i(k)\, e^{-2\sigma_i^2 k^2}\, e^{-2R_{as_i}/\lambda}}{kR_{as_i}^2} \sin\left[2kR_{as_i} + \alpha_{as_i}(k)\right] \qquad (3)$$

where N_i is the number of scatterers in the ith shell, F_i is the photoelectron backscattering amplitude of the ith shell, $-2\sigma^2 k^2$ is the Debye–Waller factor which accounts for thermal vibration and static disorder, σ is the mean-square variation in the absorber–scatterer distance R_{as_i}, λ is the mean-free path length for the photoelectron and $\alpha_{as_i}(k)$ is the net phase shift in the photoelectron wave during scattering. The sum is taken over all shells of scatterers, where a shell consists of

some number of undistinguishable atoms at approximately the same distance from the absorber.

The EXAFS data were analysed by curve-fitting. Each absorber–scatterer pair contributed with a sine-wave to the overall EXAFS. The contribution from each shell can either be calculated or determined empirically. The empirical approach to curve-fitting is to measure the amplitude and phase of the EXAFS in a model compound of known structure. These parameters are then assumed to be transferable to the compounds of interest. The model compound is chosen such that there is only a single shell of atoms contributing to each peak in the Fourier transform. Fourier filtering techniques were used to isolate the shell of interest. A six-parameter function was fitted to the measured EXAFS for the model compounds [39–41]. This parameterised function was then used as a reference when fitting the EXAFS of the unknown samples. When fitting the unknowns the number of scatterers and the absorber–scatterer distance were adjusted as variable parameters. All curve-fitting was based on a least-squares minimisation using k^3-weighted data. Data reductions and analyses were performed by the computer program XFPAKG [42].

Results

In the radial distribution function, RDF, obtained by LAXS, Fig. 2, there is a peak at 2.55 Å corresponding to the Mg–Br distance. Another peak at 1.5 Å corresponds to the intramolecular bond distances in the diethyl ether molecule [43]. A shoulder at 3.6 Å indicates a Br–Br distance with an n value of about 0.25. This corresponds to the presence of 50% of the dimeric form, $(RMgX)_2$. It was possible to carry out least-squares refinements on the Mg–Br and Br–Br interactions by assuming an octahedral configuration around magnesium. When a tetrahedral model was used only the Mg–Br distance could be refined. The Mg–O and Mg–C bond distances were set to 2.20 and 2.15 Å, respectively, in the octahedral model, and to 2.15 and 2.05 Å in the tetrahedral. These distances were estimated from the structures of the hydrated magnesium ion in aqueous solution [44], solid ethylmagnesium bromide diethyl etherate [7] and from calculated ionic radii of the magnesium ion in different configurations [45]. The Br–C and Br–O distances were calculated from the refined Mg–Br distance. The number of Mg–Br distances was refined and the number of Mg–O distances was set to 3.5 according to the amount of dimer present. The parameters of the octahedral and tetrahedral models are summarised in Table 3. The fits with an octahedral model are significantly better than with a tetrahedral model (see Figs. 1 and 2). The shoulder at 3.6 Å cannot be accounted for on the basis of a tetrahedral model and is seen as a peak in the difference curve (see Fig. 2b). The 2.0 M phenylmagnesium bromide diethyl ether solution thus contains 55% dimeric and 45% monomeric species. Magnesium is octahedrally coordinated in the dimeric structure, and it is assumed that the monomer is also octahedral, but this was not proved in the present study.

The EXAFS spectra of all the solutions are very similar, differing only very slightly in phase (Fig. 3). This indicates that the structures are the same for all the compounds, with small differences in the distances. Spectra of different data sets for the same solutions have also been compared and found to be identical. This shows that the data are consistent. The EXAFS k-space spectra were Fourier transformed

Table 3

Interatomic distances, d (Å), temperature factor coefficients, b (Å^2), and the number of distances per magnesium atom, n, for the phenylmagnesium bromide solution studied; errors derived from the least-squares refinements are given in parentheses

Model	Conc. (M)	Dimerisation (%)	d(Mg–Br)	b(Mg–Br)	n(Mg–Br)	d(Br–Br)	b(Br–Br)	n(Br–Br)	d(Br–C)	b(Br–C)	n(Br–C)
Oct.	2.0	55	2.56(2)	0.019(2)	1.55(5)	3.62(3)	0.005	0.27(5)	3.38	0.020	0.55
Tetr.	2.0	55	2.82(2)	0.009(2)	1.55	4.18	0.020	0.28	3.89	0.020	0.55

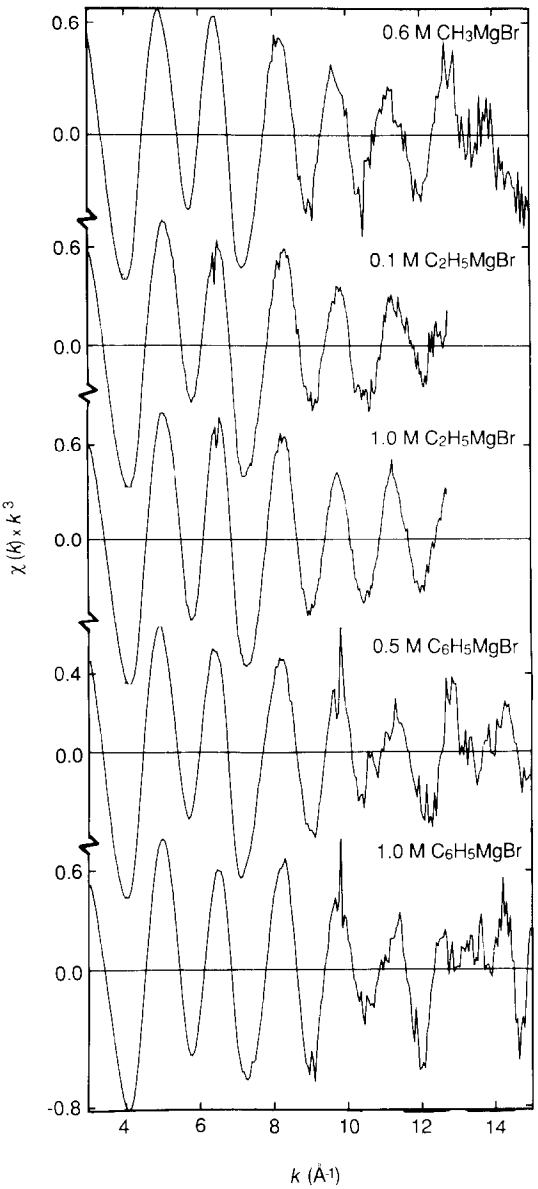

Fig. 3. EXAFS, $\chi(k)$, multiplied by k^3 vs k of organomagnesium bromides in diethyl ether solution.

to real space using a k-window of either 3–12.7 or 3–14.5 $Å^{-1}$, broadened by a Gaussian of width 0.1 $Å^{-1}$.

The Fourier transforms all show one major peak. This peak corresponds to the expected Br–Mg distance around 2.55 Å.

Curve-fitting technique was used to analyse the EXAFS data. Empirical phase and amplitude parameters for magnesium backscattering were extracted from NaBr. Fourier filtering was used to isolate the first shell. Fig. 4. The filter limits are indicated by bars on the transform. A wider filter was also applied to see if there

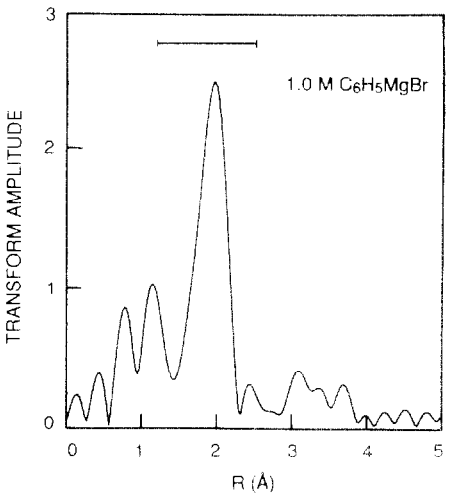

Fig. 4. Fourier transforms of k^3-weighted EXAFS data of 1 *M* phenylmagnesium bromide in diethyl ether solution, *k*-range 3.0–14.5 $Å^{-1}$. The horizontal bars indicate the width of the windows used when back-transforming the data. *R* is related to the true distance *R'* by the phase shift α according to $R' = R + \alpha$.

Table 4

EXAFS curve-fitting results of organomagnesium bromides in diethyl ether solution

Compound	Conc. (*M*)	Mg–Br distance (Å)	
		$k = 3–12.7$ ($Å^{-1}$)	$k = 3–14.5$ ($Å^{-1}$)
CH_3MgBr	0.6	2.53	2.56
C_2H_5MgBr	0.1	2.54	2.58
	1.0	2.54	
C_6H_5MgBr	0.5	2.55	2.56
	1.0	2.54	2.54

was any contribution from a Br–Br interaction and if such a wave could be fitted. This was not the case. The results from the curve-fitting are presented in Table 4. The fits gave an average Mg–Br distance of ca 2.55 Å for the phenylmagnesium bromide which is in very close agreement with the results obtained from the LAXS measurement. This shows that the phase parameters extracted from NaBr give reliable results when used in fitting Mg backscattering.

Discussion

The LAXS study of phenylmagnesium bromide in diethyl ether has given a Mg–Br distance of 2.56 Å and a Br–Br distance of 3.62 Å (Fig. 2). The intensity of the Br–Br peak corresponds to 0.5 Br–Br distances per magnesium when 55% of the Grignard reagent is present as dimers. From this value a dimerisation constant $K_{di} = [(C_6H_5MgBr)_2][C_6H_5MgBr]^{-2}$ of 0.7 M^{-1} is obtained. The value of K_{di} is in

agreement with values found for methyl-, ethyl- and phenyl-magnesium iodides in diethyl ether solution [17].

As can be seen from Fig. 3, all the EXAFS spectra for the organomagnesium bromides are very similar. Some difference in the structural details was perhaps expected, since this study covers several different R groups and various concentrations. The absence of significant variation in the results was also noted in a LAXS study of the iodides [17].

The Fourier transforms show a single peak corresponding to a distance of ca 2.55 Å (Fig. 4 and Table 4). This value is in agreement with the Mg–Br bond distance found in the LAXS measurement; 2.56(2) Å. The coordination numbers could not be determined by curve-fitting, possibly owing to a discrepancy in the Debye–Waller factor which has not been accounted for. However, both static disorder and thermal vibrations for the two absorber–scatterer pairs, in the model and sample, should be about the same.

In a dimeric species a Br–Br distance of ca 3.6 Å would be expected. The LAXS study shows that there is an appreciable amount of dimer present in diethyl ether solution, at least in the more concentrated solution, and it should be possible to detect the Br–Br interaction in the EXAFS data. Data were initially collected out to $k = 13$ Å^{-1}, but since no Br–Br interaction was observed the data range was increased to $k = 15$ Å^{-1}; however, again no Br backscattering was observed. A possible explanation for the absence of Br backscattering may be that the LAXS technique is more sensitive to long and more diffuse distances than the EXAFS technique. The information about a distance R Å from another atom enters the theoretical intensity function of LAXS by a factor $(\sin sR)/sR$ [31] and in the EXAFS equation by $(\sin 2kR)\, e^{-2r/\lambda}/R^2$, eq. 3. An X-ray scattering experiment covers the s-region 0–16 Å^{-1}, while EXAFS covers the region $6 \leqslant 2k \leqslant 30$ Å^{-1}. Thus, there is better resolution when detecting nearest neighbour environment in the EXAFS technique but it suffers from the lack of low-k data, i.e. information about long range order is lost. The signal from shells beyond the first falls off more quickly in EXAFS than in LAXS. EXAFS has the advantage that much more dilute samples can be studied.

In an earlier LAXS study of organomagnesium iodides in diethyl ether there was no indication of the presence of MgI_2 [17]. These LAXS data resemble those for phenylmagnesium iodide, and there seems to be no $MgBr_2$ present. This implies that the extended Schlenk equilibrium, eq. 2, is shifted to the left, with RMgX and $(RMgX)_2$ predominating for organomagnesium iodide and bromide in diethyl ether solution.

In tetrahydrofuran solution magnesium iodide has been shown to have dissociated into mainly MgX^+ and X^- [46]. This indicates that the concentration of MgX_2 is low in this solvent and that the Schlenk equilibrium must be coupled to the dissociation equilibrium of the magnesium halide. In more poorly solvating solvents, such as diethyl ether, where MgX_2 does not dissociate, no MgX_2 complex, and therefore no Schlenk equilibrium, has been observed by structural methods. The dissociation constant of MgX_2 is large (the formation constant of MgX_2 is small) in THF. This means that the Schlenk equilibrium can be shifted to the right even if the formation constant, $K_{\text{Schlenk}} = [MgX_2][R_2Mg][RMgX]^{-2}$, is small. These results indicate that the Schlenk equilibrium exists and that the equilibrium constant K_{Schlenk} is small. The formation of R_2Mg and MgX_2 species depends on the degree

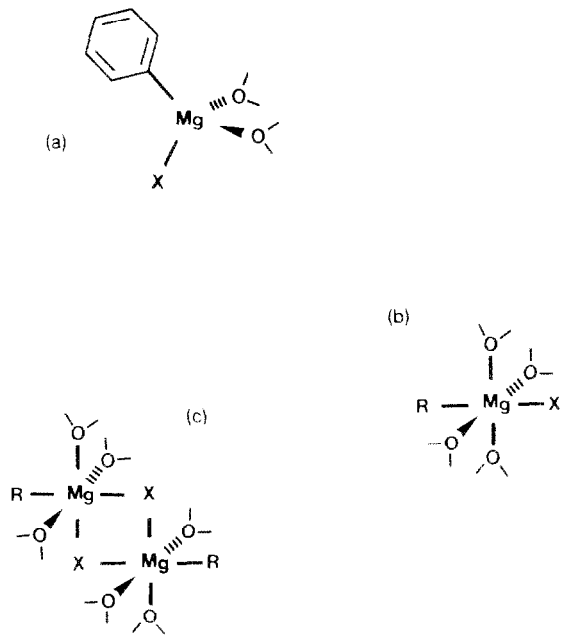

Fig. 5. Solid diethyl ether-solvated phenylmagnesium bromide has the monomeric, tetrahedral structure (a), [6]. In solution magnesium is octahedrally coordinated in the monomeric (b) as well as in the dimeric complex (c).

of dissociation of MgX_2 and the extended Schlenk equilibrium, eq. 2, must therefore be expanded even further:

$$(RMgX)_2 \rightleftharpoons 2\ RMgX \rightleftharpoons R_2Mg + MgX_2 \qquad (4)$$

$$\Vert$$

$$Mg^{2+} + 2\ X^- \rightleftharpoons MgX^+ + X^-$$

The existence of the Schlenk equilibrium was claimed to have been demonstrated by a ^{25}Mg NMR study in which it was assumed that $MgBr_2$ dissolved in THF is undissociated [14]. If it is assumed instead that $MgBr^+$ is the predominant species, the data obtained lead to the equilibrium system shown above in eq. 4. It seems reasonable to assume that $MgBr^+$ is the predominant species in view of the fact that the shift of the '$MgBr_2$' species is very close to that of the hydrated magnesium(II) ion used as reference. A neutral $MgBr_2$ complex would have a shift closer to that for other uncharged magnesium complexes with σ-bonds.

Organomagnesium bromides and iodides are present both as monomers and dimers in diethyl ether solution. Magnesium is six-coordinate in these complexes, Fig. 5. Magnesium coordinates one organic group via carbon, one halide ion and four solvent molecules in the monomeric complex, and one organic group, two bridging halide ions and three solvent molecules in the dimer. The proportion of dimer present depends on the organic group, the solvent and the concentration of

the Grignard reagent. The extent of the dimerisation in a certain solution is given by the dimerisation constant $K_{di} = [(RMgX)_2][RMgX]^{-2}$. The values of K_{di} range between 0.2 and 0.8 M^{-1} [17]. The dimerisation constant is fairly low, but the amount of dimeric species in these solutions can never be neglected and has to be taken into account even for dilute solutions of Grignard reagents.

This study has shown that the LAXS technique is useful in determining the structures of the Grignard reagents in solution, and compares favourably with spectroscopic methods. It should be possible to detect a Br–Br interaction of ca 3.6 Å in EXAFS data since the dimeric complex is probably quite rigid. If experimental conditions were changed an improvement in the data might be achieved.

Acknowledgments

This work was supported by the Swedish Natural Science Research Council. The EXAFS measurements were performed at the Stanford Synchrotron Radiation Laboratory, which is supported by the US Department of Energy, Office of Basic Energy Sciences, Division of Chemical Sciences; and the National Institutes of Health, Biomedical Resource Technology Program, Division of Research Resources. XFPAKG was kindly provided by Prof. R.A. Scott. The Knut and Alice Wallenberg Foundation is acknowledged for support of the LAXS instrument. A.W. thanks Prof. K.O. Hodgson for financial support and for providing the experimental facilities at Stanford University. Dr Britt Hedman's help in performing the experiments is greatfully acknowledged.

Note added in proof. A crystallographic study of THF solvated Grignard compounds has shown six-coordinate magnesium ions [47], which further supports octahedral configuration around magnesium in solvated Grignard compounds.

References

1 J. March, Advanced Organic Chemistry, 3rd ed., John Wiley & Sons New York, 1985.
2 H. Yamataka, Y. Kawafuji, K. Nagareda, N. Miyano and T. Hanafusa, J. Org. Chem., 54 (1989) 4706 and references therein.
3 M. Lasperas, A. Perez-Rubalcaba and M.L. Quiroga-Feijoo, Tetrahedron, 36 (1980) 3403.
4 S.G. Smith, Tetrahedron Lett., 409 (1963).
5 W. Schlenk and W. Schlenk, Ber., 62 (1929) 920.
6 G.D. Stucky and R.E. Rundle, J. Am. Chem. Soc., 86 (1964) 4825.
7 L.J. Guggenberger and R.E. Rundle, J. Am. Chem. Soc., 90 (1968) 5375.
8 J. Toney and G.D. Stucky, Chem. Commun., (1967) 1168.
9 F. Schröder and H. Spandau, Naturwissenschaften, 53 (1966) 360.
10 M. Vallino, J. Organomet. Chem., 20 (1969) 1.
11 F.W. Walker and E.C. Ashby, J. Am. Chem. Soc., 91 (1969) 3845.
12 W.V. Evans and F.H. Lee, J. Am. Chem. Soc., 55 (1933) 1474.
13 R.M. Salinger and H.S. Mosher, J. Am. Chem. Soc., 86 (1964) 1782.
14 R. Benn, H. Lehmkuhl, K. Mehler and A. Rufinska, Angew. Chem., Int. Ed. Engl., 23 (1984) 543.
15 D.F. Evans and G.V. Fazakerley, J. Chem. Soc., (1971) 184.
16 D.C. Koningsberger and R. Prins (Eds.), X-ray Absorption, John Wiley and Sons, New York, 1988; M. Magini, G. Licheri, G. Piccaluga, G. Paschina and G. Pinna (Eds.), X-ray Diffraction of Ions in Aqueous Solution: Hydration and Complex Formation, CRC Press, Cleveland, OH, 1988.
17 A. Wellmar and I. Persson, J. Organomet. Chem., 415 (1991) 155.
18 G. Johansson, Acta Chem. Scand., 20 (1966) 553.

19 I. Persson, M. Sandström, P.L. Goggin and A. Mosset, J. Chem. Soc., Dalton Trans., (1985) 1597.
20 B.E. Warren, X-ray Diffraction, Addison–Wesley, Reading, MA, 1969, Ch. 10.
21 J. Krogh-Moe, Acta Crystallogr., 9 (1956) 951.
22 N. Norman, Acta Crystallogr., 10 (1957) 370.
23 International Tables of Crystallography, Kynoch Press, Birmingham, UK, Vol. 3, 1968, and Vol. 4, 1974.
24 R.F. Stewart, E.R. Davidsson and W.T. Simpson, J. Chem. Phys., 42 (1965) 3175.
25 D.T. Cromer and J.B. Mann, J. Chem. Phys., 47 (1967) 1892.
26 D.T. Cromer, J. Chem. Phys., 50 (1969) 4857.
27 A.H. Compton and S.K. Allison, X-ray in Theory and Experiment, von Nostrand–Reinhold, New York, 1935.
28 G. Breit, Phys. Rev., 27 (1926) 362.
29 P.A.M. Dirac, Proc. R. Soc. London, 4 (1926) 195.
30 G. Johansson, Acta Chem. Scand., 25 (1971) 2787.
31 M. Sandström and G. Johansson, Acta Chem. Scand., Ser. A, 31 (1977) 132.
32 H.A. Levy, M.D. Danford and A.H. Narten, Data Collection and Evaluation with X-ray Diffractometer Designed for the Study of Liquid Structure, Report ORNL-3690, Oak Ridge National Laboratory, Oak Ridge, 1966.
33 G. Johansson and M. Sandström, Chem. Scr., 4 (1973) 195.
34 M. Molund and I. Persson, Chem. Scr., 25 (1985) 197.
35 C. Morrel, J.T.M. Baines, J.C. Campbell, G.P. Diakun, B.R. Dobson, G.N. Greaves and S.S. Hasnain, Daresbury Laboratory Synchrotron Radiation Source's EXAFS Users' Manual, 1988.
36 R.A. Scott, J.E. Hahn, S. Doniach, H.C. Freeman and K.O. Hodgson, J. Am. Chem. Soc., 104 (1982) 5364.
37 J.F. Ahlberg, E.N. Nilsson and J.L. Walsh, The Theory of Splines and Their Application, Academic Press, New York, 1967.
38 F.W. Lytle, D.E. Sayers and E.A. Stern, Phys. Rev. B, 11 (1975) 4825.
39 S.P. Cramer and K.O. Hodgson, Prog. Inorg. Chem., 25 (1979) 1.
40 S.P. Cramer, J.H. Dawson, K.O. Hodgson and L.P. Hager, J. Am. Chem. Soc., 100 (1978) 7282.
41 T.K. Eccles, Doctoral Thesis, Stanford University, USA, 1977.
42 EXAFS data analysis software package, T.K. Eccles, Stanford University and R.A. Scott, University of Georgia.
43 M. Hayashi and K. Kuwada, Bull. Chem. Soc. Jpn., 47 (1974) 3006.
44 R. Caminiti, G. Licheri, G. Piccaluga and G. Pinna, J. Appl. Crystallogr., 12 (1979) 34.
45 R.D. Shannon, Acta Crystallogr., Sect. A, 32 (1976) 751.
46 A. Wellmar and I. Persson, J. Organomet. Chem., 415 (1991) 143.
47 P.R. Markies, G. Schat, S. Griffioen, A. Villena, O.S. Akkerman, F. Bickelhaupt, W.J.J. Smeets and A.L. Spek, Organometallics, 10 (1991) 1531.